FINITE ELEMENT FOR BUCKLING OF CURVED BEAMS AND SHELLS WITH SHEAR

By Zdeněk P. Bažant,[1] M. ASCE and Mahjoub El Nimeiri[2]

INTRODUCTION

Inclusion of shear deformations allows the bending theory to be extended to relatively thick beams and shells and, at the same time, simplifies the finite element formulation for both thick and thin beams because monotonic convergence may be achieved without ensuring continuity of displacement derivatives between adjacent elements. Consequently, one may use low order interpolation polynomials, including linear ones. This is particularly useful in the case of curved beams because with higher order interpolation polynomials it is very difficult to satisfy exactly the conditions of no self-straining at rigid body rotations and of availability of all constant strain states (2,3,6,10), while with linear displacement interpolation polynomials and a straight shape of the element these requirements are easily met.

As the beam depth, d (or cylindrical shell thickness), becomes very small keeping the element length, l, constant, the contribution of shear stiffness to the element stiffness matrix must vanish. However, this was found not to occur, a condition which was termed "spurious shear stiffness" (20) and was shown to be responsible for ill-conditioning of the stiffness matrix in the case of very slender beams or thin cylindrical shells. A number of remedial techniques have been proposed (7,8,9,11,12,14,15,16,17,18,20,21). Best known is the technique of reduced numerical integration (1,20) which, however, does not allow the use of linear interpolation polynomials. In a recent work (7) (not covering buckling and curved beams) it has been shown that the ill-conditioning (or spurious shear stiffness) can also be avoided if the actual plate thickness, d, is replaced by a modified thickness, d', depending on the element size, l. However, this could hardly be applied in the case of irregular cross sections (e.g., I, T, and box) or nonhomogeneous and layered cross sections.

In a recent study (5), the writers found that the problem of spurious shear stiffness also arises in the combined Saint-Venant and warping torsion of box girders, but can be eliminated by introducing a new formulation in which the degree, N_d, of interpolation polynomials for transverse displacements (and twist) is $N_r - 1$, N_r being the degree of polynomials for longitudinal displacements

Note.—This paper is part of the copyrighted Journal of the Structural Division, Proceedings of the American Society of Civil Engineers, Vol. 101, No. ST9, September, 1975. Manuscript was submitted for review for possible publication on March 28, 1974.

[1]Prof. of Civ. Engrg., Northwestern Univ., Evanston, Ill.

[2]Struct. Analyst, Joslyn Manufacturing & Supply Co., Woodstock, Ill.; formerly, Grad. Student, Northwestern Univ., Evanston, Ill.

(rotation and warping). (This is contrary to the general practice of using $N_d = N_r + 1$.) It was also observed (5) that this formulation can eliminate the problem of spurious shear in bending of slender beams or cylindrical shells, but the formulation for this case was not developed in detail. This will be done herein, showing a new formulation which is particularly useful for curved beams. All analysis will be restricted to deformations in the plane of curvature.

INTERPOLATION POLYNOMIALS AND INCREMENTAL STIFFNESS MATRIX

A curved beam will be approximated by a series of straight elements [Fig. 1(*a*)] with skew ends satisfying full continuity between elements. For best

TABLE 1.—Numerical Results

Type of problem (1)	SIMPLY SUPPORTED BEAM: (a) Midspan Deflection, in inches (2)	(3)	(4)	(5)	(6)	(7)	(b) Euler Buckling Load, in 10^7 pounds (8)	(9)	(10)	CIRCULAR RING: (c) Deflection, in inches, Under load (11)	Horizontal (12)	(d) q_{cr}, in 10^5 pounds (13)	(14)	ARCH: (e) Circular Arch, q_{cr}, in 10^5 pounds (15)	(16)
l/b	16	16	16	16	16	40	4	16	32	16	16	16	32	16	32
δ_2/δ_1	10	1	0.5	0.1	0	1	1	1	1	1	1	1	1	1	1
$n = 8$							92.00	11.12							
$n = 16$	0.1703	1.232	1.884	3.283	4.264		91.62	9.60		1.489	1.279	4.892	0.637	2.113	2.750
$n = 32$	0.1716	1.307	2.066	3.861	5.014	22.637	91.61	9.02	2.408	1.580	1.357	4.635	0.586	2.003	2.530
$n = 80$						25.413	91.61	8.92	2.331						
$n = 96$	0.1720	1.331	2.127	4.072	5.288					1.609	1.382	4.553	0.570	1.968	2.467
Exact	0.1720	1.333	2.133	4.102	5.333	25.638	91.61	8.92	2.321	1.611	1.384	4.547	0.568	1.966	2.456

Note: 1 in. = 25.4 mm; 1 lb = 0.4536 kg.

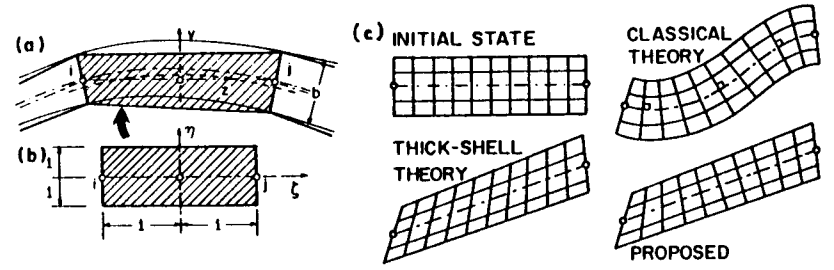

FIG. 1.—(*a*) Subdivision of Beam in Finite Elements; (*b*) Mapping from Unit Parent Element; (c) Comparison of Displacement Interpolation Functions

accuracy, the axis of each element is chosen to deviate equally to both sides from the given curved axis [Fig. 1(*a*)]. The element will be conveniently visualized as a mapped image of a parent unit rectangular element [Figs. 1(*a*) and 1(*b*)]. By virtue of the straightness of element, the mapping is linear in each coordinate, i.e.

$$z = \frac{1}{4}(1-\zeta)(-l + b_{z_i}\eta) + \frac{1}{4}(1+\zeta)(l + b_{z_j}\eta) \quad \ldots\ldots\ldots\ldots\ldots\ldots (1a)$$

$$y = \frac{1}{4}(1-\zeta)\, b_{y_i}\eta + \frac{1}{4}(1+\zeta)\, b_{y_j}\eta \quad \ldots\ldots\ldots\ldots\ldots\ldots\ldots\ldots (1b)$$

in which z, y = local rectangular coordinates of the element centered at midlength of the element [Fig. 1(*a*)]; l = length of element; ζ, η = coordinates of the parent rectangular element that are mapped into z and y; subscripts i, j refer to the ends of element; b_{z_i}, b_{y_i} (or b_{z_j}, b_{y_j}) = components of vector $\mathbf{b}$ that characterizes the orientation of the cross section, such that $b = |\mathbf{b}|$ represents the depth [or thickness, Fig. 1(*a*)] of the beam (which may vary along the beam). The mapping in Eq. 1*a* is introduced in such a form that $\zeta = \pm 1$ are the end cross sections and, in the case of doubly symmetric cross section, $\eta = \pm 1$ are the top and bottom fibers of the beam element; for an asymmetric cross section, the limits are $\eta_2 = 2y_2/b$ and $\eta_1 = \eta_2 - 2$, in which y_2 = y-coordinate of the top fiber measured from the centroid. The displacements, u and v, in z and y directions will be considered to be distributed as:

$$u = \frac{b}{2}\left[(\zeta^2-\zeta)\Phi_i + (1-\zeta^2)\Phi_0 + (\zeta^2+\zeta)\Phi_j\right]\eta + \frac{1}{2}(1-\zeta)U_i + \frac{1}{2}(1+\zeta)U_j \quad \ldots\ldots\ldots\ldots\ldots\ldots (2a)$$

$$v = \frac{1}{2}(1-\zeta)V_i + \frac{1}{2}(1+\zeta)V_j \quad \ldots\ldots\ldots\ldots\ldots\ldots\ldots\ldots (2b)$$

Φ = rotation of cross section; V = transverse deflection; U = longitudinal displacement of the centroid; and subscript 0 refers to the midlength of element (interior node). In contrast to the usual finite elements for bending (13), the distribution of deflection, v, is not cubic but linear, and in contrast to the usual thick-shell finite elements (19), the polynomials for u and v are not of the same degree [Fig. 1(*c*)], and the element is not isoparametric but subparametric (19).

Consider now that the beam is initially in equilibrium at initial normal stresses $\sigma_z^0 = P^0/A$, due to initial axial force P^0 and initial shear stresses τ_{zy}^0. Subsequently, an infinitesimal incremental deformation occurs. The virtual work of stresses $(\sigma_z^0 + \sigma_z)$ and $(\tau_{zy}^0 + \tau_{zy})$ after incremental deformation upon any kinematically admissible variation $\delta u(z, y)$, $\delta v(z, y)$ is $\delta W = \delta W_1 + \delta W_0 - \int_z (q_z \delta u + q_y \delta v)dz$ with

$$\delta W_1 = \int_z\int_A \sigma_z\, \delta e_z\, dA dz + \int_z\int_A \tau_{zy}\, \delta e_{zy}\, dA dz \quad \ldots\ldots\ldots\ldots\ldots (3)$$

$$\delta W_0 = \int_z\int_A \sigma_z^0\, \delta \epsilon_z\, dA dz + \int_z\int_A \tau_{zy}^0\, \delta \gamma_{zy}\, dA dz \quad \ldots\ldots\ldots\ldots\ldots (4)$$

in which A = area of cross section; q_z, q_y = load components per unit length of beam; and

$$e_z = \frac{\partial u}{\partial z}; \quad \epsilon_z = e_z + \frac{1}{2}\left(\frac{\partial v}{\partial z}\right)^2 \quad \ldots\ldots\ldots\ldots\ldots\ldots\ldots\ldots (5)$$

$$e_{zy} = \frac{\partial u}{\partial y} + \frac{\partial v}{\partial z}; \quad \gamma_{zy} = e_{zy} + \frac{1}{2}\frac{\partial v}{\partial y}\frac{\partial v}{\partial z} \quad \ldots\ldots\ldots\ldots\ldots\ldots\ldots (6)$$

in which e_z, e_{zy} = small (linearized) normal and shear strains; and ϵ_z, γ_{zy} = finite normal and shear strains. Eq. 3 contains linearized strain because only infinitesimal incremental deformation is considered. Nevertheless, in the product $\sigma_z^0\, \delta\epsilon_z$ (Eq. 4) the finite strain expression must be used, because, in view of σ_z^0 and τ_{zy}^0 being finite (large), the product, $\sigma_z^0\, \delta e_z$, would be accurate only up to small quantities of first order in displacement gradients, whereas the product, $\sigma_z\, \delta e_z$ (Eq. 3), is a small quantity of second order (4). Component $(\partial u/\partial z)^2$ has been deleted from ϵ_z since for small incremental strains it is negligible with regard to e_z. Similar comments can be made about $\tau_{zy}\, \delta e_{zy}$ and $\tau_{zy}^0\, \delta\gamma_{zy}$.

It is expedient to introduce the column matrices

$$\mathbf{e} = (e_z, e_{zy})^T, \underline{\sigma} = (\sigma_z, \tau_{zy})^T \quad \ldots\ldots\ldots\ldots\ldots\ldots\ldots\ldots (7)$$

$$\mathbf{q} = (U_i, V_i, \Phi_i, U_j, V_j, \Phi_j, \Phi_0)^T = (\mathbf{q}^{bT}, \Phi_0)^T \quad \ldots\ldots\ldots\ldots\ldots (8)$$

$$\mathbf{q}^b = (U_i, V_i, \Phi_i, U_j, V_j, \Phi_j)^T \quad \ldots\ldots\ldots\ldots\ldots\ldots\ldots (9)$$

in which superscript T denotes a transpose. Then

$$\underline{\sigma} = \mathbf{D}\,\mathbf{e}, \mathbf{e} = \mathbf{B}\,\mathbf{q}; \quad \mathbf{B} = \mathbf{a}\,\mathbf{d}\,\mathbf{b} \quad \ldots\ldots\ldots\ldots\ldots\ldots\ldots (10)$$

in which $\mathbf{D}$ = (2 × 2) elastic matrix defined as $D_{ij} = 0$ for $i \neq j$; D_{11} = E = Young's modulus; $D_{22} = G$ = shear modulus (modified by the shear correction coefficient for a given shape of cross section); $\mathbf{B}$ = (2 × 7) matrix; and matrices $\mathbf{a}$, $\mathbf{d}$, and $\mathbf{b}$ are defined by

$$\mathbf{e} = \mathbf{a}\,\mathbf{u}'; \quad \mathbf{u}' = \mathbf{d}\,\hat{\mathbf{u}}; \quad \hat{\mathbf{u}} = \mathbf{b}\,\mathbf{q} \quad \ldots\ldots\ldots\ldots\ldots\ldots\ldots (11)$$

in which $\mathbf{u}' = (\partial u/\partial z, \partial u/\partial y, \partial v/\partial z)^T$;

$$\hat{\mathbf{u}} = (\partial u/\partial\zeta, \partial u/\partial\eta, \partial v/\partial\zeta, \partial v/\partial\eta)^T \quad \ldots\ldots\ldots\ldots\ldots (12)$$

Further, it is useful to set

$$\frac{\partial v}{\partial z} = \mathbf{d}'\left(\frac{\partial v}{\partial\zeta}, \frac{\partial v}{\partial\eta}\right)^T = \mathbf{d}'\,\mathbf{b}'\,\mathbf{q} = \mathbf{C}\,\mathbf{q} \quad \text{with} \quad \mathbf{C} = \mathbf{d}'\,\mathbf{b}' \quad \ldots\ldots\ldots (13)$$

Matrices $\mathbf{b}'$ and $\mathbf{d}'$ are easily derived from the relation

$$\begin{Bmatrix} \frac{\partial u}{\partial\zeta} \\ \frac{\partial u}{\partial\eta} \end{Bmatrix} = \begin{bmatrix} \frac{\partial z}{\partial\zeta}, & \frac{\partial y}{\partial\zeta} \\ \frac{\partial z}{\partial\eta}, & \frac{\partial y}{\partial\eta} \end{bmatrix} \begin{Bmatrix} \frac{\partial u}{\partial z} \\ \frac{\partial u}{\partial y} \end{Bmatrix} = \mathbf{J} \begin{Bmatrix} \frac{\partial u}{\partial z} \\ \frac{\partial u}{\partial y} \end{Bmatrix} \quad \ldots\ldots\ldots\ldots (14)$$

in which $\mathbf{J}$ = Jacobian matrix of the mapping defined by Eq. 1, and from a similar relation that holds for the derivatives of v. Denoting by J_{ij}^{-1} the components of the inverse matrix, $\mathbf{J}^{-1}$, one obtains

$$\mathbf{d} = \begin{bmatrix} J_{11}^{-1} & J_{12}^{-1} & 0 & 0 \\ J_{21}^{-1} & J_{22}^{-1} & 0 & 0 \\ 0 & 0 & J_{11}^{-1} & J_{12}^{-1} \end{bmatrix}; \quad \mathbf{d}' = [J_{11}^{-1}, J_{12}^{-1}] \quad \ldots\ldots\ldots (15)$$

Using Eqs. 11, 13, 8, and 9, Eqs. 3 and 4 can be brought to the forms $\delta W_1 = \int_z \int_A \delta \underline{\epsilon}^T \underline{\sigma}\, dz dA = \delta \mathbf{q}^T \mathbf{K}^1 \mathbf{q}$ and $\delta W_0 = \int_z \int_A \sigma_z^0 (\mathbf{C}\delta\mathbf{q})^T \mathbf{C}\, \mathbf{q}\, dz dA = \delta \mathbf{q}^T \mathbf{K}^0 \mathbf{q}$ in which

$$\mathbf{K}^1 = \int_z \int_A \mathbf{B}^T \mathbf{D}\, \mathbf{B}\, dz dA = \int_{-1}^{1} \int_{\eta_1}^{\eta_2} \mathbf{B}^T \mathbf{D}\, \mathbf{B}\, |J|\, d\eta d\zeta \quad \ldots\ldots\ldots (16)$$

$$\mathbf{K}^0 = \frac{P^0}{A} \int_{-1}^{1} \int_{\eta_1}^{\eta_2} \mathbf{C}^T \mathbf{C}\, |J|\, d\eta d\zeta \quad \ldots\ldots\ldots (17)$$

where $\mathbf{K}^1$, $\mathbf{K}^0$ = stress-independent and stress-dependent parts of incremental stiffness matrix $\mathbf{K}$; $|J|$ = det ($\mathbf{J}$). Terms that do not involve $\mathbf{q}$ have been deleted in δW_0 because they do not affect the stiffness.

The virtual work may now be expressed as $\delta W = \delta \mathbf{q}^T (\mathbf{K}^1 \mathbf{q} + \mathbf{K}^0 \mathbf{q} - \mathbf{F})$, in which $\mathbf{F}$ = (7 × 1) column matrix of applied forces associated with $\mathbf{q}$. The condition that δW vanish for any $\delta \mathbf{q}$ yields the incremental equilibrium condition of the element

$$\mathbf{K}\,\mathbf{q} = \mathbf{F} \quad \text{with} \quad \mathbf{K} = \mathbf{K}^1 + \mathbf{K}^0 \quad \ldots\ldots\ldots (18)$$

in which $\mathbf{F}$ are applied forces associated with $\mathbf{q}$ (Eq. 9). The last row of matrix in Eq. 18 refers to Φ_0. Since Φ_0 is a rotation of an internal node, it may be eliminated from the system of equations (which is termed "static condensation" of stiffness matrix) (13). This yields the condensed equilibrium equation of the element

$$\mathbf{k}\,\mathbf{q}^b = \mathbf{f} \quad \text{with} \quad \mathbf{k} = \mathbf{k}^1 + \mathbf{k}^0 \quad \ldots\ldots\ldots (19)$$

in which $\mathbf{k}^1$, $\mathbf{k}^0$ are the parts arising from $\mathbf{K}^1$, $\mathbf{K}^0$. Note that matrix $\mathbf{k}^0$ is obtained from $\mathbf{K}^0$ merely by deleting zero rows and zero columns associated with the internal node.

In the general case, the stiffness matrix is best computed from Eqs. 16 and 17 by Gaussian-point integration (8 points were used). In the special case of a straight beam of constant cross section, the nonzero components of the upper triangular part of the symmetric (6 × 6) matrix $\mathbf{k}^1$ are

$$k_{11}^1 = \frac{EA}{l},\ k_{14}^1 = -k_{11}^1,\ k_{22}^1 = (60\, EI_x + GA_w l^2)(6l^3\psi_y)^{-1};\quad k_{23}^1 = -\frac{l}{2} k_{22}^1,$$

$$k_{25}^1 = -k_{22}^1,\ k_{26}^1 = k_{23}^1;\quad k_{33}^1 = [(80 + 24\psi_y)\, EI_x + 3GA_w l^2](24l\psi_y)^{-1};$$

$$k_{35}^1 = (60\, EI_x + GA_w l^2)(12l^2\psi_y)^{-1},\ k_{36}^1 = [(40 - 24\psi_y) EI_x$$

$$- GA_w l^2](24l\psi_y)^{-1};\quad k_{44}^1 = k_{11}^1,\ k_{55}^1 = k_{22}^1,\ k_{56}^1 = -k_{23}^1,\ k_{66}^1 = k_{33}^1 \quad \ldots\ldots (20)$$

in which A_w = area of the webs; and $\psi_y = 1 + 10\, EI_x (GA_w l^2)^{-1}$. The geometric stiffness matrix, $\mathbf{k}^0$ (6 × 6 in size), has, in the present formulation, a simpler form than it has in the usual formulation and its only nonzero elements are $k_{22}^0 = k_{55}^0 = P^0/l$, $k_{25}^0 = k_{52}^0 = -k_{22}^0$.

Numerical Examples

To examine the convergence with growing number n of identical elements, beams, rings, and arches of various slenderness ratios have been solved numerically. The results are summarized in Table 1. In all cases the cross section was a hollow square box, constant along the beam, of width b = 120 in. (3.048 m), depth $d = b$; Young's modulus $E = 30 \times 10^6$ psi (206.8 kN/mm^2), shear modulus $G = E/3$; thickness δ_1 = 1 in. (25.4 mm) of the walls parallel to axis y. Various thicknesses δ_2 of horizontal walls were considered. The exact solutions in Table 1 were solved from the differential equations for bending or buckling of beams with shear deformation.

In case a, a simply supported beam of span L is loaded by moments 4×10^7 lb × in. (4.519 MN × m) at both ends. In case b, Table 1 gives axial buckling load of the beam. In cases $c - d$ a ring of perimeter $2L$ is stretched by two opposite loads $P = 10^6$ lb (453,590 kg) acting along the diameter, and Table 1 gives the deflection under load, w_1, as well as the deflection along a horizontal diameter which is perpendicular to the load direction, w_2. In case e, Table 1 gives the critical uniformly distributed radial load, q_r, for the first antisymmetric plane buckling mode of a circular two-hinge arch of length L (along the curve) and of central angle 60°.

Analysis of Results and Conclusions

Examples show that the convergence is monotonic, i.e., upper bound solutions are guaranteed. This is due to the fact that a fully consistent finite element formulation characterized by full continuity between the elements is used. In the case of very slender beams, the rate of convergence is found to be distinctly slower than that for the usual slender beam elements with cubic displacement variation, and so a higher number of elements is needed, which is naturally expected because of the assumed linear variation of the displacements. But for deep beams the convergence is very fast. The convergence rate improves considerably as the thickness of top and bottom flanges increases and the shear deformation of the vertical webs becomes more important, whereas for a slender solid rectangular beam without flanges (case $\delta_2 = 0$ in Table 1), in which the shear deformation is not too pronounced, the rate of convergence is poor.

The source of poor convergence in the case of very slender beams may be clarified by considering the matrix in Eq. 20 for a solid rectangular cross section of depth d. When $d \to 0$ (very slender beam) while keeping l, E, and G fixed, the effect of shear stiffness, GA_w, should vanish for the spurious shear stiffness phenomenon to be absent, and all stiffness coefficients except the axial ones (EA/l) should decrease as d^3, i.e., k_{ij}^1/d^3 must be finite as $d \to 0$. But examination of Eq. 20, in which $GA_w \sim d$, $EI_x \sim d^3$, $\lim \psi_y = 1$, and $GA_w l^2 \sim d$ ($\sim$ denoting proportional dependence), reveals that $k_{ij}^1/d^3 \to \infty$ as $d \to 0$. At the same time, however, it appears from this consideration that $\lim k_{ij}^1/d^3$ can be made finite by substituting $G = 0$ in all elements of the matrix in Eq. 20 except in coefficient ψ_y. In this manner, the spurious stiffness phenomenon is easily eliminated. (This is done, of course, at the expense of loosing monotonous convergence, i.e., upper-bound solutions.) Furthermore, it has been verified numerically that the substitution of $G = 0$ except in ψ_y

also greatly improves accuracy, even for rather deep beams. Apparently, the shear is adequately accounted for by coefficient ψ_y, the other terms due to shear being unrealistic.

When the stiffness matrix is calculated by numerical integration, the foregoing elimination of shear corresponds to the following procedure: (1) Calculate the diagonal stiffness coefficient, K^1_{77}, associated with interior node rotation Φ_0, separately for $E = 1$, $G = 0$ and for $E = 0$, $G = 1$, and express K^1_{77} as $\alpha E + \beta G$; (2) calculate $\psi_y = 1 + \alpha E/\beta G$ for actual E and G; and (3) expressing K^1_{77} as $\beta G\ \psi_y$, replace here and in all other terms of the row and column associated with Φ_0 the actual value of G by a very small number, e.g., $G = 10^{-25}$; then proceed to calculate the rest of K^1_{ij} and condense K^1_{ij}.

Note the special role of the interior node rotation in eliminating the spurious shear phenomenon. Apparently, the additional degree of freedom associated with this node (and resulting from the fact that $N_r = N_d + 1$) makes it possible for the excess equilibrium condition associated with this node to enforce in the limit for $d \rightarrow 0$ the normality of cross section in a certain average sense within the element. Further, note that the spurious shear stiffness could also be eliminated by setting $G = 0$ at the outset (giving $\psi_y = 1$); but for deep beams the accuracy would then be poor.

Finite elements of the type proposed are particularly expedient in the case of curved beams. The reason is that the interpolation (shape) functions in Eq. 2 enable the ends of element to be made skew with regard to its axis, so that one may easily achieve full continuity between finite elements, as well as fulfill the conditions of no self-straining in rigid body rotation and of availability of all constant strain states. These conditions are very difficult to satisfy exactly with curved finite elements based on the classical bending theory (2,3,6,10).

Finite elements with various other combinations of the interpolation polynomials for displacements (degree N_d) and for rotation (degree N_r) have been examined. Among all other possible combinations of the degrees $N_d = 1, 2, 3$ and $N_r = 1, 2, 3$, only the case $N_d = 2$, $N_r = 3$ allows a similar elimination of spurious shear stiffness by merely deleting the shear terms. Accuracy for slender beams was in this case also much better than that shown in Table 1, but the formulation was cumbersome in the case of curved beams. It seems that in general the ease of elimination of spurious shear stiffness requires that

$$N_d = N_r - 1 \qquad (21)$$

It was also found that, after applying static condensation to the three interior nodes needed for the case $N_d = 2$, $N_r = 3$, the stiffness matrix is identical to that derived in a different manner by Prziemieniecki (p. 80 of Ref. 13) for prismatic beams without initial forces.

Appendix.—References

1. Ahmed, S., Irons, B. M., and Zienkiewicz, O. C., "Analysis of Thick and Thin Shell Structures by Curved Finite Elements," *International Journal for Numerical Methods in Engineering*, Vol. 2, 1970, pp. 419-451.
2. Ashwell, D. G., Sabir, A. B., and Roberts, T. M., "Further Studies in the Application of Curved Finite Elements to Circular Arches," *International Journal of Mechanical Sciences*, Vol. 13, 1971, pp. 507-517.
3. Austin, W. J., "In-Plane Bending and Buckling of Arches," *Journal of the Structural

Division, ASCE, Vol. 97, No. ST5, Proc. Paper 8130, May, 1971, pp. 1575-1592.
4. Bažant, Z. P., "A Correlation Study of Formulations of Incremental Deformation and Stability of Continuous Bodies," *Transactions of the American Society of Mechanical Engineers, Journal of Applied Mechanics*, Vol. 38, 1971, pp. 919-928.
5. Bažant, Z. P., and ElNimeiri, M., "Stiffness Method for Curved Box Girders at Initial Stress," *Journal of the Structural Division*, ASCE, Vol. 100, No. ST10, Proc. Paper 10877, Oct., 1974, pp. 2071-2090.
6. Dawe, D. J., "Finite Deflection Analysis of Arches," *International Journal for Numerical Methods in Engineering*, Vol. 3, 1971, pp. 529-552.
7. Fried, I., "Shear in C^0 and C^1 Bending Finite Elements," *International Journal of Solids and Structures*, Vol. 9, 1973, pp. 449-460.
8. Greimann, L. F., and Lynn, P. P., "Finite Element Analysis of Plate Bending with Transverse Shear Deformation," *Nuclear Engineering and Design*, Vol. 14, 1970, pp. 223-230.
9. Irons, B. M., and Razzague, A., "Experience with the Patch Test for Convergence of Finite Elements," *The Mathematical Foundations of the Finite Element Method*, A. K. Aziz, ed., Academic Press, New York, N.Y., 1972, pp. 557-587.
10. Megard, G., "Planar and Curved Shell Elements," *Finite Element Methods in Stress Analysis*, I. Holand and K. Bell, eds., Tapir-T.U., Trondheim, Norway, 1970, pp. 287-318.
11. Melosh, R. J., "A Flat Triangular Shell Element Stiffness Matrix," *Proceedings of the Conference on Matrix Methods in Structural Mechanics*, Air Force Institute of Technology, Wright-Patterson Air Force Base, Dayton, Ohio, 1965.
12. Pryor, C. W., and Baker, R. M., "A Finite Element Analysis Including Transverse Shear Effects for Applications to Laminated Plates," *American Institute of Aeronautics and Astronautics Journal*, Vol. 9, 1971, pp. 912-917.
13. Przemieniecki, J. S., *Theory of Matrix Structural Analysis*, McGraw-Hill Book Co., Inc., New York, N.Y., 1968.
14. Severn, R. T., "Inclusion of Shear Deflection in the Stiffness Matrix for a Beam Element," *Journal of Strain Analysis*, Vol. 5, 1970, pp. 239-241.
15. Stricklin, J. A., et al., "A Rapidly Converging Triangular Plate Element," *American Institute of Aeronautics and Astronautics Journal*, Vol. 7, 1969, pp. 180-181.
16. Wempner, G. A., "Finite Elements, Finite Rotations and Small Strains of Flexible Shells," *International Journal of Solids and Structures*, Vol. 5, 1969, pp. 117-153.
17. Wempner, G. A., Oden, J. T., and Kross, D. A., "Finite Element Analysis of Thin Shells," *Journal of the Engineering Mechanics Division*, ASCE, Vol. 94, No. EM6, Proc. Paper 6259, Dec., 1968, pp. 1273-1294.
18. Utku, S., "Stiffness Matrices for Thin Triangular Elements of Non-Zero Gaussian Curvature," *American Institute of Aeronautics and Astronautics Journal*, Vol. 5, 1967, pp. 1659-1667.
19. Zienkiewicz, O. C., *The Finite Element Method in Engineering Science*, McGraw-Hill Book Co. Ltd., London, England, 1971.
20. Zienkiewicz, O. C., Taylor, R. L., and Too, J. M., "Reduced Integration Techniques in General Analysis of Plates and Shells," *International Journal for Numerical Methods in Engineering*, Vol. 3, 1971, pp. 255-290.
21. Zudans, Z., "Analysis of Asymmetric Stiffened Shell Type Structures by the Finite Element Method-III. Constant Transverse Shear Model," *Nuclear Engineering and Design*, Vol. 11, 1970, pp. 177-194.